EasyChair Preprint

№ 3474

Economic Model Predictive Control of Organic Rankine Cycle Based Waste Heat Energy Conversion Systems

Shawn Li, Kang Li, Mingming Lin, Jinzhu Pu and Jianhua Zhang

May 23, 2020

Economic model predictive control of organic Rankine cycle based waste heat energy conversion systems

Shawn LI[a], Kang LI[a], Mingming LIN[b], Jinzhu PU[c] and Jianhua ZHANG[c]

[a] *University of Leeds, Leeds, UK, k.li1@leeds.ac.uk*
[b] *Qingdao University of Science and Technology, Qingdao, China, linmm1232008@126.com*
[c] *North China Electric Power University, Beijing, China, zjhncepu@163.com*

Abstract:
Organic Rankine cycle (ORC) has been widely used in low-grade waste heat recovery. Besides the safety and effectiveness issues, the economic operation and control of Organic Rankine cycle (ORC) systems have is becoming increasingly important. In this paper, an economic model predictive controller (EMPC) is developed, which directly uses an economic index of the organic Rankine cycle (ORC) system as the controller objective and realizes the economic optimization while maintaining the dynamic tracking performance. Compared with the traditional two-layer supervisory control, two main contributions can be achieved: (1) The online dynamic optimization is achieved which maximizes the unit net power recovery; (2) The single-layered architecture further enhances the real-time control performance and reduces the complexity of controller design. The numerical simulation results confirm the efficacy of the proposed controller design, meeting the industrial requirements while decreasing the payback time of the upfront installation costs.

Keywords:
Economic model predictive control, Energy consumption reduction, Economic efficiency, Organic Rankine Cycle, Waste heat recovery

1. Introduction

Reducing energy consumption while improving energy efficiency in industrial processes have attracted renewed interests in recent years. Waste energy recovery (WER) plays an important role in improving the energy efficiency of the production process. In this regard, up to 50% energy consumption is wasted globally in the form of heat due to the lack of cost-effective waste heat recovery (WHR) systems and the limitation of heat recovery rate [1]. Majority of low grade heat sources within the range from 50 Celsius degree up to 350 Celsius degree are from industrial processes, household heating, exhaust gases from the combustion engines, solar and geothermal radiation [2, 3]. Similar to the conventional steam Rankin cycle (SRC) [1], organic Rankine cycle (ORC) replaces water-based working fluid with organic compound, in order to increase the waste heat recovery efficiency and reduce system size. As substantial efforts have been invested in the organic working fluid selection [4–6] and architecture optimization [7–9], ORC is poised to be a promising technique to effectively convert waste heat sources into electricity.

In order to guarantee the operating efficiency, safety and durability, controller design is indispensable in ORC based WHR system operation. In general, there are two operating scenarios [10]. When the ORC is feeding electricity directly to the loads without a power converter interface, the generated electricity has to follow the load variations, namely following the connected load (FCL) mode [11]. On the other hand, if a full-capacity converter interface is integrated between ORC and grid, the amount of produced electricity is able to follow the thermal source variations to achieve maximum energy conversion rate. Under this circumstance,

the control objective of ORC aims to maximize the conversion efficiency over the thermal source fluctuations, i.e. following the utilized thermal energy (FTE) mode [12]. Compared with FCL mode, the controller design for FTE mode is more challenging. Two independent proportional-integral (PI) control loops were employed in [13]. Though fast controlling action can be achieved on the pump using the feedforward control (FFC), the control performance degrades when the operating condition deviates from the nominal operation points. Besides, the gain scheduling control (GSC) method was applied to FTE mode over the specific range of operating conditions [14]. Under this circumstance, less energy consumption has been reported compared with the PI control. In [15], the ORC based WHR system was formulated by a complex physical model. As a result, when controlling such a plant, the impact of the nonlinearity, uncertainty and disturbances of the thermal source has to be considered in real time. Therefore, a constrained model predictive control based real-time optimal control strategy was employed in [12], in which a multi-variable model was simplified via the application of the controlled auto-regressive integrated moving average (CARIMA) technique [11, 12], which was parameterised using the recursive least square (RLS) method. The varying working conditions were considered to obtain a satisfactory control performance. For all the aforementioned control paradigms, the optimal steady-state setting point is set in the upper control layer [16,17], namely the real-time optimization (RTO). In the hierarchical control scheme, RTO performs steady-state optimization based on the knowledge of economic performance and updates these set-points periodically [18]. The prescribed setting points will steer the actuators in the lower layer to control the variables to their steady states while rejecting the dynamic disturbances [16,17]. However, due to the hierarchical structure, information exchange between different layers causes delays, and the control performance will degrade whenever the system operation conditions vary fast. For the FTE mode, the objective function used by the controller in [12] prioritizes on the tracking behaviours and outputs variance attenuation while coping with disturbances. As a result, the objective function does not consider the economic issue while the ORC plant aims to capture the maximum thermal energy. In fact, the set-points of controlled ORC may vary in real-time due to the changes in the inlet mass flow rates and the temperatures from the waste heat source [10].

In this paper, a newly proposed economic model predictive controller (EMPC) is adopted to maximize the energy conversion rate in real-time. EMPC is a variant of MPC, which combines the two control layers into single layer, forcing the process to converge to the economically optimal steady-state. Therefore, the controller has been simplified and more waste thermal heat can be converted to electricity compared with the conventional MPC method. In this work, the similar CARIMA model and RLS parameterization tool have been adopted. Furthermore, a terminal constraint [19, 20] has been employed to construct the EMPC controller to guarantee stability. Finally, the simulation results confirm the efficacy of the proposed method.

2. Process description

The schematic diagram of the investigated FTE mode ORC plant in this work is shown in Fig.1. The configuration of the ORC system is straightforward to implement, as there is no connected external drum for the water stream, and the used organic working fluid in this paper is R245fa. The variable flow rate and temperature of the inlet waste heat gases are used to heat and vaporize the organic fluid in the evaporator. The high pressure vapor is then directed to the expander to drive the expander to convert thermal energy into mechanical energy. Then, the working fluid in the gas state is condensed and converted back into liquid state by an air-cooled condenser. The connected reservoir will store the condensed working fluid and then it will be pressurised by the pump. In the end, the pressurised working fluid will flow through the evaporator to begin a new cycle.

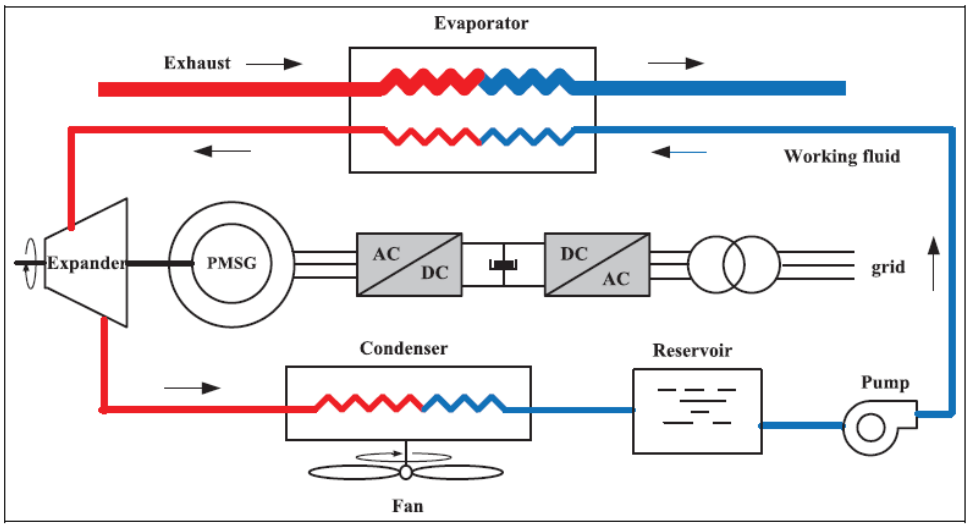

Figure 1: The schematic diagram of the investigated FTE mode ORC plant [10]

3. ORC model construction and parameter identification

3.1. State space formulation

In this work, similar to [15], a three-input and four-output multivariable physical model is employed to describe the ORC system. Therein, the manipulated variables (MV) of the system are rotating speed of pump N_p, rotating speed of expander N_{exp}, and mass flow rate of cooling air $\dot{m}_c$. On the other hand, the output controlled variables (CV) are overall system power output W which is a significant modification compared with the previous research [12], evaporating pressure P_e, superheating temperature T_{su}, and the condenser outlet temperature T_c. For a neat expression, the overall system is thus interpreted by the following state-space equation:

$$\dot{x}(t) = f(x(t), u(t), v(t)) \tag{1}$$

where $u = [N_p \quad N_{\text{exp}} \quad \dot{m}_c]^T$ is the MV vector, and $v = [\dot{m}_{\text{ai}}, T_{\text{ai}}]^T$ is regarded as the disturbance vector, in which $\dot{m}_{\text{ai}}$ and T_{ai} are the mass flow rate and temperature of the exhaust gas at the inlet of the evaporator respectively. The state vector x is expressed as below. The notation definitions are detailed in Table 1

$$x = [L_1, L_2, P_e, h_o, T_{w1}, T_{w2}, T_{w3}, T_{a1}, T_{a2}, T_{a3}, L_{c1}, L_{c2}, P_c, h_{co}, T_{cw1}, T_{cw2}, T_{cw3}] \tag{2}$$

The output equation is expressed as follows:

$$y(t) = h(x(t), u(t), v(t)) \tag{3}$$

where the CVs are $y(t) = [P_e,\ T_{su},\ T_c]^T$.

3.2. Model Identification

Later, the controlled auto-regressive integrated moving average (CARIMA) model is employed to reproduce the dynamics of the ORC process as follows:

$$A\left(z^{-1}\right) y(t) = B\left(z^{-1}\right) u(t-1) + D\left(z^{-1}\right) v(t-1) + \frac{1}{\Delta} C\left(z^{-1}\right) \epsilon(t) \tag{4}$$

where $A(z^{-1})$, $B(z^{-1})$ and $D(z^{-1})$ are polynomial matrices. The model parameters of the above equation can be estimated using the well-established recursive least squares algorithm (RLS) with fixed forgetting factor, where more details can be referred to [11, 12].

Table 1: Notations for state vector

L	length of region [m]
P	pressure [kPa]
h	specific enthalpy [J/kg]
T	temperature [K]
Subscripts	
1	unsaturated liquid region
2	liquid-vapor mixture region
3	superheated vapor region
e	evaporator
o	outlet
w	wall
a	exhaust gas
c	condenser

4. EMPC design for ORC plant

Firstly, the general formulation scheme of EMPC is introduced as follows:

$$\begin{aligned}
&\min_{u\in S(\Delta)} \int_0^{\tau_N} l_e(\tilde{x}(t), u(t))dt \\
&\text{subject to} \quad \dot{\tilde{x}}(t) = f(\tilde{x}(t), u(t), 0) \\
&\tilde{x}(0) = x(\tau_k) \\
&g(\tilde{x}(t), u(t)) \leq 0, \quad \forall t \in [0, \tau_N)
\end{aligned} \tag{5}$$

where $l_e(x, u)$ is the economic cost function, $\tilde{x}(t)$ is the state prediction given manipulated variable $u(t)$ and 0 disturbances, and $g(x, u)$ is other constraints imposed on the system.

In order to secure the stability, EMPC scheme is commonly incorporated with other assumptions or constraints. In this work, terminal constraints $V_f(\tilde{x}(N))$ [20] is applied and Eq.5 can be reformulated in the form of discretization time space as follows:

$$\begin{aligned}
&\min_{u(0),\ldots,u(N-1)} \sum_{j=0}^{N-1} l_e(\tilde{x}(j), u(j)) + V_f(\tilde{x}(N)) \\
&\text{subject to} \quad \tilde{x}(j+1) = f_d(\tilde{x}(j), u(j), 0) \\
&\tilde{x}(0) = x(k) \\
&\tilde{x}(N) \in \mathbb{X}_f \\
&(\tilde{x}(j), u(j)) \in \mathbb{Z}, \quad \forall j \in \mathbb{I}_{0:N-1}
\end{aligned} \tag{6}$$

where $\tilde{x}$ is the predicted state under the assumption of no disturbance imposed on the system and f_d represents the discretized system formulation. $\mathbb{Z} = \mathbb{X}_f \times \mathbb{U}$ is a compact feasibility region, which is equivalent to g in the continuous case.

4.1. Economic cost

The energy conversion efficiency of ORC under the FTE mode was introduced in [12]. According to the previous investigation [15], the net work output is given by:

$$w_{\text{net}} = \int_{t_1}^{t_2} (W - W_p)dt \tag{7}$$

where W_p is the pump consumption power, and W is the system output power. Then the following assumptions are applied:

- Due to the fast dynamics of the generator, the system output power is assumed to be equal to the expander work for simplicity:

$$W = \dot{w}_{\text{exp}} \tag{8}$$

- The energy consumption of pump is assumed to be a constant.

Hence, in order to optimize the net work output with stable inputs, the objective function is derived in the discrete time-space:

$$\max_{\Delta u(0),\ldots,\Delta u(N-1)} \alpha \sum_{j=0}^{N-1} W(t+j|t) - \sum_{j=1}^{M} \Delta u(t+j-1)^T R \Delta u(t+j-1) \tag{9}$$

where R is the weight matrix for input smoothness penalty, N and M are prediction horizon and control horizon respectively, and α is the weight for output power.

4.2. Terminal constraints design

For the stability consideration, the terminal constraints are imposed on the EMPC objective function described above:

$$\begin{aligned}\min_{\Delta u(0),\ldots,\Delta u(N-1)} & \left[\hat{y}(t+N|t) - \tilde{y}(t+N)\right]^T Q \left[\hat{y}(t+N|t) - \tilde{y}(t+N)\right] \\ & + \left(\sum_{j=1}^{M} \Delta u(t+j-1)^T R \Delta u(t+j-1)\right) - \alpha \left(\sum_{j=0}^{N-1} W(t+j|t)\right)\end{aligned} \tag{10}$$

where Q is the terminal stability weight matrix. In other words, the system output, i.g. the converted electricity, is maximized along the path and also the terminal output values of the prediction window $\hat{y}(t+N|t)$ are forced to converge to the steady-state reference values $\tilde{y}(t+N)$.

4.3. Constrained EMPC with measurable disturbances

The cost function is described in Eq.10. In order to maintain the primary ORC process variables within the operating limitations, constraints are imposed on manipulated variables and controlled variables. For MVs, the natural upper and lower bounds and safe operating constraints are:

$$-\Delta u_{\max} \leq \Delta u(t) \leq \Delta u_{\max} \tag{11}$$

$$u_{\min} \leq u(t) \leq u_{\max} \tag{12}$$

where $\Delta u_{\max}$ is maximum rate of the control input, $u_{\min}$ and $u_{\max}$ are minimum and maximum input values, respectively. Analogous to the MVs, constraints have to be applied to CVs for safety consideration:

$$y_{\min} \leq y(t) \leq y_{\max} \tag{13}$$

where $y_{\min}$ and $y_{\max}$ are the minimum and maximum output values respectively.

Based on the Diophantine equation and polynomial matrix calculations in [12], the j-step prediction output can be obtained as follows:

$$\hat{y}(t+j|t) = G_j\left(z^{-1}\right)\Delta u(t+j-1) + f_j \tag{14}$$

where $f_j = G_{jp}(z^{-1}) + H_{jp}(z^{-1})\Delta v(t-1) + F_j(z^{-1})y(t)$. Considering a set of j ahead predictions in Eq.14, the multi-horizon prediction equation is expressed as

$$\hat{\mathrm{Y}}(t) = \mathrm{G}\Delta\mathrm{U}(t) + \mathrm{f}(t) \tag{15}$$

where

$$\mathrm{G} = \begin{bmatrix} G_0 & 0 & \cdots & 0 & \cdots & 0 \\ G_1 & G_0 & \cdots & 0 & \cdots & 0 \\ \vdots & \vdots & \ddots & \vdots & \vdots & \vdots \\ G_{j-1} & G_{j-2} & \cdots & G_0 & \vdots & 0 \\ \vdots & \vdots & \vdots & \vdots & \ddots & \vdots \\ G_{N-1} & G_{N-2} & \cdots & \cdots & \cdots & G_0 \end{bmatrix}, \quad \mathrm{f}(t) = \begin{bmatrix} f_1 \\ f_2 \\ \cdots \\ f_j \\ \cdots \\ f_{N_y} \end{bmatrix},$$

$$\Delta\mathrm{U}(t) = \begin{bmatrix} \Delta u(t) \\ \Delta u(t+1) \\ \cdots \\ \Delta u(t+j-1) \\ \cdots \\ \Delta u(t+M-1) \end{bmatrix}, \quad \hat{\mathrm{Y}}(t) = \begin{bmatrix} \hat{y}(t+1|t) \\ \hat{y}(t+2|t) \\ \cdots \\ \hat{y}(t+j|t) \\ \cdots \\ \hat{y}(t+N|t) \end{bmatrix}$$

Substituting the prediction Eq.15 into the objective function Eq.10, the cost function can be reformulated as:

$$J = \frac{1}{2}\Delta\mathrm{U}^T(t)\mathrm{K}\Delta\mathrm{U}(t) + \mathrm{g}^T\Delta\mathrm{U}(t) + C \tag{16}$$

where $\mathrm{K} = 2[\mathrm{G}^T\bar{\mathrm{Q}}\mathrm{G}+\bar{\mathrm{R}}]$, $\mathrm{g} = \mathrm{G}^T[2\bar{\mathrm{Q}}(\mathrm{f}(t)-\tilde{\mathrm{y}}(t+1))+\bar{\mathrm{B}}]$, and $C = [\mathrm{f}(t)-\tilde{\mathrm{y}}(t+1)]^T\bar{\mathrm{Q}}[\mathrm{f}(t)-\tilde{\mathrm{y}}(t+1)]+\bar{\mathrm{B}}^T\mathrm{f}(t)$. Moreover, $\bar{\mathrm{Q}}$, $\bar{\mathrm{R}}$, and $\bar{\mathrm{B}}$ are multi-window matrices created based on single-window matrices Q, R, and value α:

$$\bar{\mathrm{Q}} = \begin{bmatrix} 0 & \cdots & 0 & 0 \\ \vdots & \ddots & \vdots & \vdots \\ 0 & \cdots & 0 & 0 \\ 0 & \cdots & 0 & Q \end{bmatrix}_{NN}, \quad \bar{\mathrm{R}} = \begin{bmatrix} R & \cdots & 0 & 0 \\ \vdots & \ddots & \vdots & \vdots \\ 0 & \cdots & R & 0 \\ 0 & \cdots & 0 & R \end{bmatrix}_{M\times M}, \quad \bar{\mathrm{B}} = \begin{bmatrix} -\alpha e_1^T \\ \vdots \\ -\alpha e_1^T \\ -\alpha e_1^T \end{bmatrix}_{N\times 1}$$

where $e_1 = [1\ 0\ 0\ 0]$. The inequalities 11, 12, and 13 can be transformed into the following compact form:

$$\mathrm{T}\Delta\mathrm{U}(k) \leq \mathrm{L} \tag{17}$$

where

$$\mathrm{T} = \begin{bmatrix} I_1 \\ -S_z \\ S_z \\ -\mathrm{G} \\ \mathrm{G} \end{bmatrix}, \quad \mathrm{L} = \begin{bmatrix} S \times \Delta u_{\max} \\ -S \cdot u_{\min} + S \cdot u(t-1) \\ S \cdot u_{\max} - S \cdot u(t-1) \\ -S_n \cdot y_{\min} + \mathrm{f}(t) \\ S_n \cdot y_{\max} - \mathrm{f}(t) \end{bmatrix}, \quad S_z = \begin{bmatrix} I_2 & & & 0 \\ I_2 & I_2 & & \\ \vdots & & & \\ I_2 & & \cdots & I_2 \end{bmatrix}_{M\times M},$$

$$S = \underbrace{[I_2, I_2, \cdots, I_2]}_{M}^T, \quad S_n = \underbrace{[I_3, I_3, \cdots, I_3]}_{N}^T$$

$$I_1 = I_{(n_u\times M)\times(n_u\times M)}, \quad I_2 = I_{n_u\times n_u}, \quad I_3 = I_{n_y\times n_y}$$

and n_u is the number of MVs, n_y is the number of CVs. In order to obtain the optimal incremental control input, the following constrained optimization problem need to be solved:

$$\min_{\Delta\mathrm{U}(t)} J = \frac{1}{2}\Delta\mathrm{U}^T(t)\mathrm{K}\Delta\mathrm{U}(t) + \mathrm{g}^T\Delta\mathrm{U}(t) + C, \quad s.t. \quad \mathrm{T}\Delta\mathrm{U}(t) \leq \mathrm{L} \tag{18}$$

5. Simulation results

The following tests have been conducted based on the ORC process model to investigate the performance of the proposed EMPC controller. Therein, the sampling rate is set to $T_s = 2s$. Both prediction horizon N and control horizon M in Eq 9 are set to $N = M = 8$. The weight matrices in Eq 10 are set to

$$Q = \begin{bmatrix} 0 & 0 & 0 & 0 \\ 0 & 20 & 0 & 0 \\ 0 & 0 & 50 & 0 \\ 0 & 0 & 0 & 200 \end{bmatrix}, \quad R = \begin{bmatrix} 0.005 & 0 & 0 \\ 0 & 0.005 & 0 \\ 0 & 0 & 0.5 \end{bmatrix}$$

It is notable that the first element in Q is set to 0 as no reference steady value for output W is applied, whereas maximizing W is the economic motivation in the EMPC controller design. The control inputs are limited in terms of $0 \leq N_p \leq 4000$ r/min and $0 \leq N_{\text{exp}} \leq 3000$ r/min. The maximum rates of two control inputs are $\Delta N_p = 100$ r/min and $\Delta N_{\text{exp}} = 100$ r/min respectively. The weight for economic cost function is set to $\alpha = 0.001$. Note that the initial settings of other variables in this work can be referred to [12]. In order to examine the disturbance rejection performance and the transient tracking behaviour, two experiments have been conduced.

5.1. Disturbance rejection test

In this test, disturbances on both the temperature and flow rate are introduced, which can be seen from Figure 2. The output power and other output variables tracking performances are shown in Fig.2 and Fig.3. It can be seen that the output power always follows the variations in the temperature and flow rate. As the output power is added in the economic cost function in EMPC scheme, it is expected to outperform the MPC counterpart. Though prescribed weight settings for the economic cost is small, EMPC still performs slightly better. The statics to measure the differences between EMPC and MPC is illustrated in Table 2, which is defined as:

$$\frac{1}{T}\sum_{j=1}^{T}\left(\hat{W}_{\text{EMPC}}(j) - \hat{W}_{\text{MPC}}(j)\right)$$

Other observations can be obtained through these experiments that CVs are bounded within appropriate range centring set-points. Additionally, MVs are also fluctuating within feasible regions.

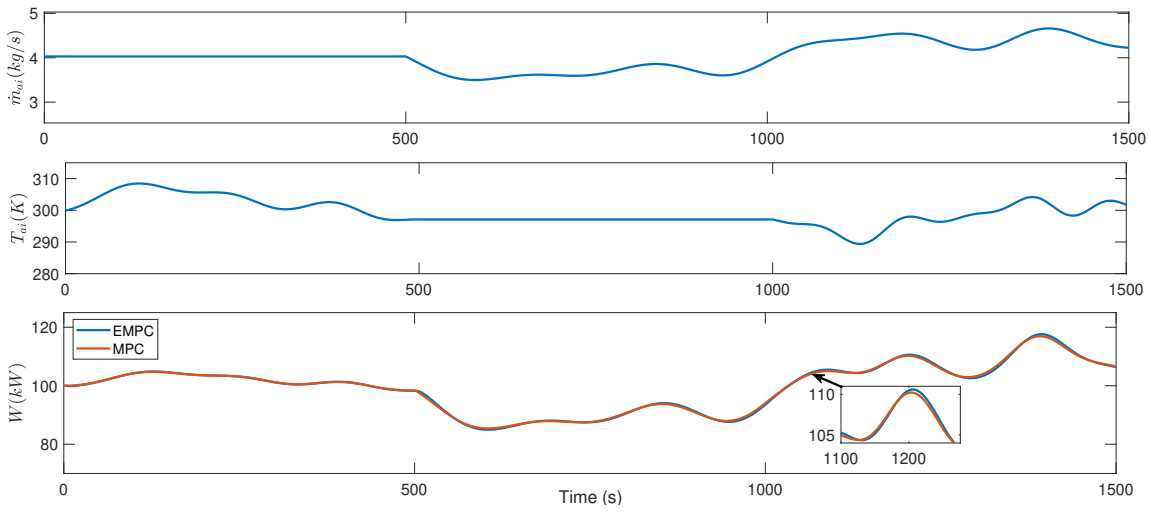

Figure 2: Disturbances and output power in disturbance rejection test

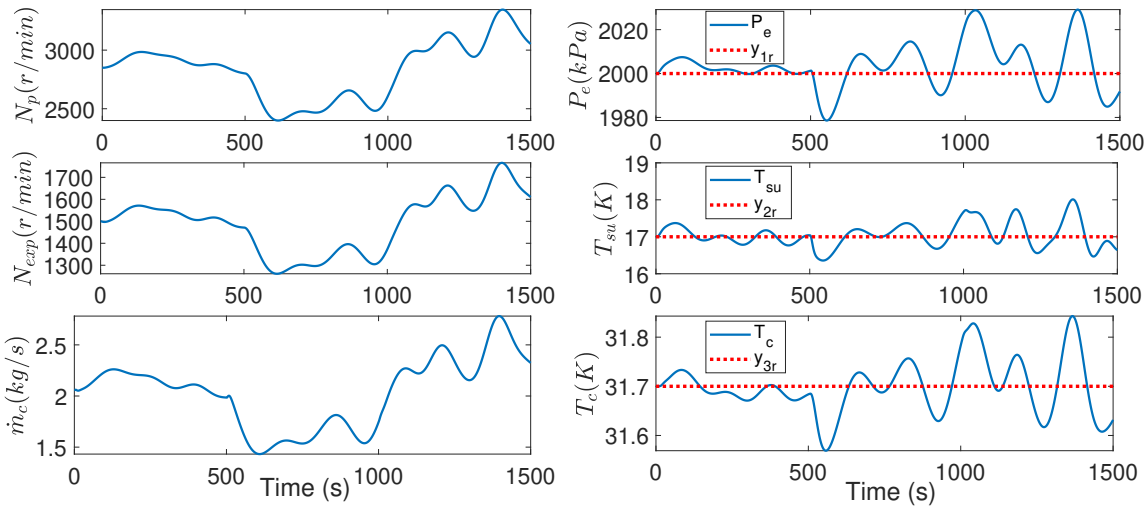

Figure 3: Evaluations of MVs and CVs in disturbance rejection test

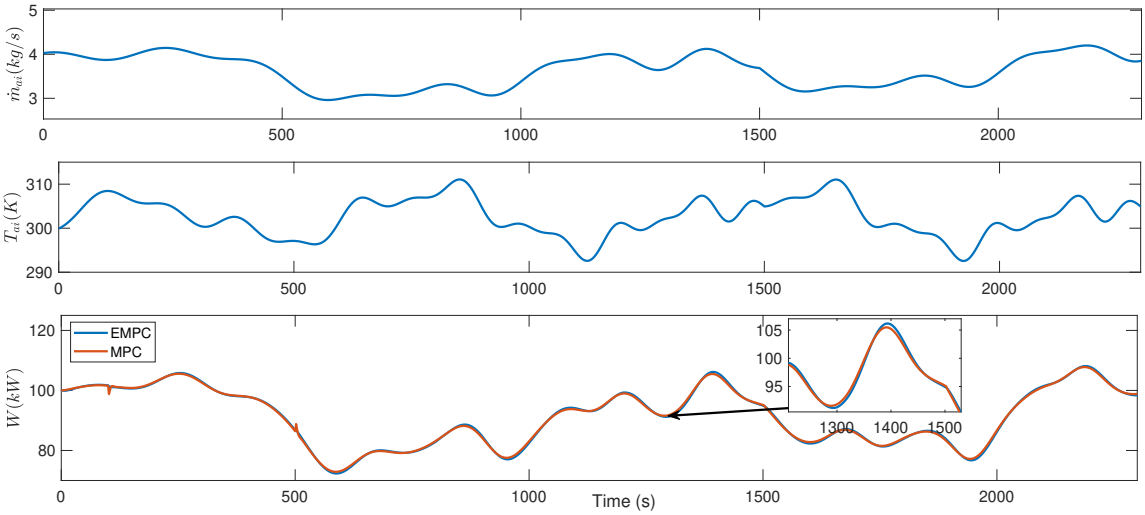

Figure 4: Disturbances and output power in set-points tracking test

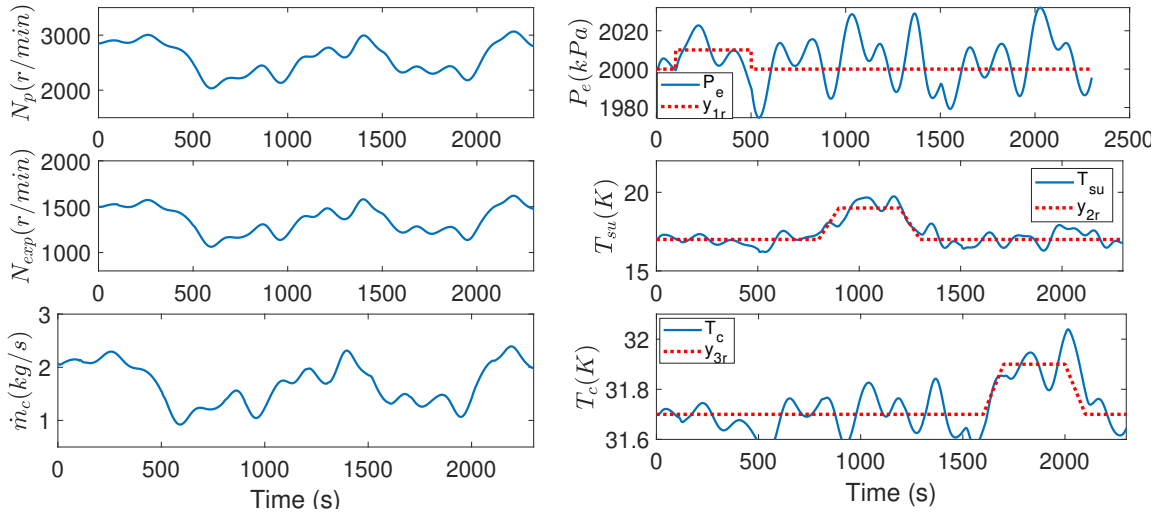

Figure 5: Evaluations of MVs and CVs in set-points tracking test

5.2. Set-point tracking test

In this section, the set-points of evaporating pressure, superheating temperature and condenser outlet temperature are changed respectively in order to test transient set-point tracking ability. Similar conclusions can be drawn based on these results in Fig.4 and Fig.5. EMPC still outperforms MPC in terms of larger output power. The quantitative measurements are given in Table 2. On the other hand, the CVs are varying within acceptable ranges centring around the changing set-points. However, the evaporating pressure seems to be the most volatile variable, where the fluctuations in percentage change are still reasonable given the large magnitude.

Table 2: EMPC outperforms MPC in output power

Simulation Mode	Disturbance Rejection	Set-point Tracking
Avg. $W_{\text{EMPC}} - W_{\text{MPC}}$ (W)	14.7133	11.5402

6. Conclusion

In this paper, the control performance of a recently proposed control strategy, namely economic model predictive control, on organic Rankine cycle based waste heat energy conversion systems, has been investigated. The EMPC method integrates the economic components into the generic objective function to realize the maximum net energy recovery from the expander. The CARIMA model and recursive least squares have been applied to map the correlations of the state and output variables. Compared with the traditional MPC method, EMPC considers the economic cost, which is not required to take the quadratic form in formulating the cost function. In order to secure good stability, terminal constraints have been introduced into the controller design. The simulation results confirm that the amount of heat recovery has increased compared to the traditional MPC. In addition, the proposed EMPC possesses good stability and disturbance rejection capability compared with the existing MPC control scheme.

Acknowledgments

This research is financially supported by the UK Engineering and Physical Sciences Research Council (EPSRC) under grant EP/P004636/1 'Optimising Energy Management in Industry' - "OPTEMIN".

References

[1] K. Rahbar, S. Mahmoud, R. K. Al-Dadah, N. Moazami, S. A. Mirhadizadeh, Review of organic rankine cycle for small-scale applications, Energy conversion and management 134 (2017) 135–155.

[2] T.-C. Hung, T. Shai, S. K. Wang, A review of organic rankine cycles (orcs) for the recovery of low-grade waste heat, Energy 22 (7) (1997) 661–667.

[3] S. Lecompte, H. Huisseune, M. Van Den Broek, B. Vanslambrouck, M. De Paepe, Review of organic rankine cycle (orc) architectures for waste heat recovery, Renewable and sustainable energy reviews 47 (2015) 448–461.

[4] J. Bao, L. Zhao, A review of working fluid and expander selections for organic rankine cycle, Renewable and sustainable energy reviews 24 (2013) 325–342.

[5] J. Larjola, Electricity from industrial waste heat using high-speed organic rankine cycle (orc), International journal of production economics 41 (1-3) (1995) 227–235.

[6] U. Drescher, D. Brüggemann, Fluid selection for the organic rankine cycle (orc) in biomass power and heat plants, Applied thermal engineering 27 (1) (2007) 223–228.

[7] S. Quoilin, M. Orosz, H. Hemond, V. Lemort, Performance and design optimization of a low-cost solar organic rankine cycle for remote power generation, Solar energy 85 (5) (2011) 955–966.

[8] V. Dolz, R. Novella, A. García, J. Sánchez, Hd diesel engine equipped with a bottoming rankine cycle as a waste heat recovery system. part 1: Study and analysis of the waste heat energy, Applied Thermal Engineering 36 (2012) 269–278.

[9] J. Sun, W. Li, Operation optimization of an organic rankine cycle (orc) heat recovery power plant, Applied Thermal Engineering 31 (11-12) (2011) 2032–2041.

[10] J. Zhang, K. Li, J. Xu, Recent developments of control strategies for organic rankine cycle (orc) systems, Transactions of the Institute of Measurement and Control 41 (6) (2019) 1528–1539.

[11] J. Zhang, Y. Zhou, Y. Li, G. Hou, F. Fang, Generalized predictive control applied in waste heat recovery power plants, Applied energy 102 (2013) 320–326.

[12] J. Zhang, Y. Zhou, R. Wang, J. Xu, F. Fang, Modeling and constrained multivariable predictive control for orc (organic rankine cycle) based waste heat energy conversion systems, Energy 66 (2014) 128–138.

[13] S. Quoilin, R. Aumann, A. Grill, A. Schuster, V. Lemort, H. Spliethoff, Dynamic modeling and optimal control strategy of waste heat recovery organic rankine cycles, Applied energy 88 (6) (2011) 2183–2190.

[14] J. Zhang, M. Lin, F. Fang, J. Xu, K. Li, Gain scheduling control of waste heat energy conversion systems based on an lpv (linear parameter varying) model, Energy 107 (2016) 773–783.

[15] J. Zhang, W. Zhang, G. Hou, F. Fang, Dynamic modeling and multivariable control of organic rankine cycles in waste heat utilizing processes, Computers & Mathematics with Applications 64 (5) (2012) 908–921.

[16] J. B. Rawlings, D. Angeli, C. N. Bates, Fundamentals of economic model predictive control, in: 2012 IEEE 51st IEEE conference on decision and control (CDC), IEEE, 2012, pp. 3851–3861.

[17] M. Ellis, H. Durand, P. D. Christofides, A tutorial review of economic model predictive control methods, Journal of Process Control 24 (8) (2014) 1156–1178.

[18] J. Zhang, M. Lin, F. Shi, J. Meng, J. Xu, Set point optimization of controlled organic rankine cycle systems, Chinese science bulletin 59 (33) (2014) 4397–4404.

[19] D. Angeli, R. Amrit, J. B. Rawlings, On average performance and stability of economic model predictive control, IEEE transactions on automatic control 57 (7) (2011) 1615–1626.

[20] R. Amrit, J. B. Rawlings, D. Angeli, Economic optimization using model predictive control with a terminal cost, Annual Reviews in Control 35 (2) (2011) 178–186.